

PROGETTAZIONE CONCETTUALE DI DISPOSITIVI ANTI-SISMICI CON CORE IN SCHIUMA DI ALLUMINIO PER CBFS

CONCEPTUAL DESIGN OF ANTI-SEISMIC DEVICES WITH METAL FOAM CORE FOR CBFS

Amparo de la Peña, Massimo Latour
Gianvittorio Rizzano
University of Salerno
Department of Civil Engineering
Fisciano, Italy
amparo.delape@gmail.com, mlatour@unisa.it
g.rizzano@unisa.it

Atsushi Sato
Nagoya Institute of Technology
Gokiso, Showa, Nagoya, Japan
sato.atsushi@nitech.ac.jp

ABSTRACT

Metal foam is a relatively new and potentially revolutionary material due to its properties such as the low weight-to-stiffness ratio, high damping and energy dissipation capacity. Even if this material is widely used in mechanical, aerospace and automotive industries, it is still not frequently used in civil engineering applications. The large energy dissipation capacity that metal foams possess could be exploited to control the seismic performance of structures, but only a few research investigations have been focused on this matter. Within this context, the present paper investigates a possible solution to realise dissipative aluminium foam dampers to be applied in X-braced steel structures resembling a concentrically braced steel frame (CBF). The bracing system consists of a steel rod or tube linked to the aluminium foam damper. The damper is constituted of aluminium foam that provides the structure with dissipation capacity when activated under compression. The permanent deformations of the aluminium foam are absorbed by a wedge device, avoiding a pinching behaviour in the global response. Analytical equations governing the global behaviour of the bracing system are herein developed. An X-braced steel frame complying with Eurocode 8 provisions is designed and considered as a case study. The structure is subsequently upgraded by introducing the dissipative device into the bracings. The results of preliminary experimental and numerical tests on the components of the device are herein presented, showing the potentiality of the solution.

SOMMARIO

La schiuma metallica è un materiale relativamente nuovo e potenzialmente rivoluzionario, grazie alle sue proprietà quali il basso rapporto peso/rigidità, l'elevato smorzamento e la capacità di

dissipare energia. Anche se questo materiale è ampiamente utilizzato nell'industria meccanica, aerospaziale e automobilistica, non è ancora utilizzato frequentemente nelle applicazioni di ingegneria civile. La grande capacità di dissipazione di energia che le schiume metalliche possiedono potrebbe essere sfruttata per controllare le prestazioni sismiche delle strutture, ma solo poche ricerche si sono concentrate su questo argomento. In questo contesto, il presente lavoro studia una possibile soluzione per realizzare dispositivi anti-sismici in schiuma di alluminio da introdurre in strutture in acciaio con controventi concentrici a croce di S. Andrea. Il sistema di controventatura è costituito da un'asta o da un tubo di acciaio collegati al dissipatore. Lo smorzatore è costituito da schiuma di alluminio che fornisce alla struttura una capacità di dissipazione quando viene attivato in compressione. Le deformazioni permanenti della schiuma di alluminio sono assorbite da un dispositivo a cuneo, che evita globalmente fenomeni di "pinching". Sono state sviluppate le equazioni analitiche che regolano il comportamento globale del sistema. Come caso di studio è stato progettato e considerato un telaio in acciaio a X conforme alle disposizioni dell'Eurocodice 8. La struttura viene successivamente adeguata introducendo il dispositivo dissipativo in controventi. Vengono presentati i risultati di prove sperimentali e numeriche preliminari sui componenti del dispositivo, che mostrano le potenzialità della soluzione.

1 INTRODUCTION

Over the past century, the materials employed for the construction of structures have been essentially limited to solid ones, most commonly steel, aluminium or composite components. However, the mechanical properties of structural steel, for instance, are difficult to improve due to physical limitations. In fact, the modulus of elasticity of steel cannot be significantly modified, while its' resistance cannot be indefinitely increased either.

Within this context, multiple research studies have been recently focusing on developing innovative materials, as they stand as an opportunity to improve the seismic performance of civil structures. Among these materials, metal foam is relatively new and potentially revolutionary. Metal foams consist of heterogeneous cells composed of a gas phase dispersed in a metallic one. The advantages of metal foams over solid metals lie in a combination of plasticity, an ultra-light structure and large energy dissipation capacity.[1]. Metal foams can be distinguished according to their method of production and their cell typology, either open or closed ones. Open-cell metal foams present low stiffness, high porosity and good thermal insulation properties. When tested in compression, open-cell foams present well-defined plateau stress after the yielding of the material, in which the cell edges yield in bending. On the other hand, closed-cell metal foams present low density (300-600 kg/m³), low heat conductivity, relatively high stiffness, fire resistance and relatively high compression/tension resistance (10-20 MPa) [2]. Unlike open-cell foams, closed-cell ones show a more complex behaviour under compression. After the yielding of the material, the foam presents plateau up to a densification strain, beyond which the structure compacts and the stress rises steeply. Thus, the energy dissipation capacity of metal foams under compression is high. Conversely, when subjected to tensile stresses, metal foams present a much lower ductility capacity [4].

The main applications of metal foams are mainly focused on the automotive, military and aerospace industries [3]-[5]. However, their mechanical properties make them also suitable for applications in structures. They are useful in cases in which minimal weight is required, as in structures in seismic zone. Moreover, they result in a convenient choice when high stiffness and resistance along with low thickness are required, as in slabs, to reduce the volumetric and environmental impact [1]. Finally, metal foams can also be used in damping applications due to their high ductility properties. Within the civil engineering field, great interest has shown the scientific community for the use of metal foams as the core component of sandwich panels or infills in hollow sections due to the great benefit in terms of buckling mitigation and shear resistance that metal foams provide [6]. The use of sandwich panels in dry floors has been recently studied in [1], where small-size tests were

performed on panels glued through thin layers of bi-component epoxy resin. Moreover, the high energy dissipation capacity in compression given by metal foams has led to their introduction in anti-seismic devices. Their insertion in structural members subjected to axial stresses was firstly studied in [7], where foam-filled tubes were investigated. A gain in efficiency was obtained in the foam-filled tube, as it was determined that the total energy absorbed could be increased up to 30% when compared to single tubes. Tubular steel elements with metallic foams were further studied in [8].

Within this framework, the objective of the work hereinafter reported is to present a set of tests aimed at further demonstrating the potentialities that derive from the application of aluminium foam material (AFM) in civil engineering. This paper presents a dissipative aluminium foam damper to be applied in X-braced steel frames. The bracing system consists of a steel rod or tube linked to the aluminium foam damper. The damper device is constituted of AFM that provides the structure with dissipation capacity when activated under compression. The permanent deformations of the AFM are absorbed by a spring-wedge device, initially proposed in [9], avoiding a pinching behaviour in the global response. The analytical equations governing the global behaviour of the bracing system are herein presented. A single-storey X-braced steel system resembling a concentrically braced frame (CBF) and complying with Eurocode 8 provisions [10] is designed and considered as a case study. The structure is subsequently upgraded by introducing the dissipative device to investigate the potentiality of the proposed solution. The results of preliminary experimental and numerical tests on the components of the device are presented, showing the potentiality of the solution.

2 ALUMINIUM FOAM DAMPER

2.1 Device's description

The proposed damper, depicted in the 3D model in Fig. 1, shall be located within the bracing elements of a CBF. The main components of the device are the aluminium foam layers, able to dissipate the incoming seismic energy, and a wedge system equipped with a spring mechanism, with the aim to absorb the permanent deformations following the seismic actions [9]. The first one is composed of a number of cylindrical AFM layers concentrically drilled with a dimension such as to accommodate the diameter of the rod (*i.e.*, brace). On the other hand, the wedge system consists of a top wedge (Fig. 2(a)) containing a threaded hole to accommodate the rod. This element is in contact with a bottom wedge that is constituted by a built-up element made up of three plates (Fig. 2(b)). The surface in contact with the bottom wedge is treated with thermally spray coating M4 [11] with the aim to obtain a friction coefficient greater than 0.6. It is characterised by an inclination of 30°. The wedge mechanism lies on a bearing plate (Fig. 2(c)) that does not only work as a support system to accommodate the movement of the bottom wedge when activated, but it also transmits the stresses developed in the rod to the aluminium metal foam layers located underneath. The bearing plate is connected to the bottom wedge through a double-spring system. Both the AFM and the wedge mechanism are placed inside an external tube welded to squared endplates in both ends. The upper endplate has a hole with dimensions such as to accommodate the rod, whereas the bottom endplate hosts not only the rod but also an inner tube that is intended to limit the interaction between the rod and the rest of the elements.

The kinematic mechanism of the damper consists of the compression of the AFM when the rod is activated in tension. The plastic deformations developed in the foam material under compression lead to a gap opening that will be subsequently filled by the activation of the wedge mechanism, with the help of pre-elongated springs.

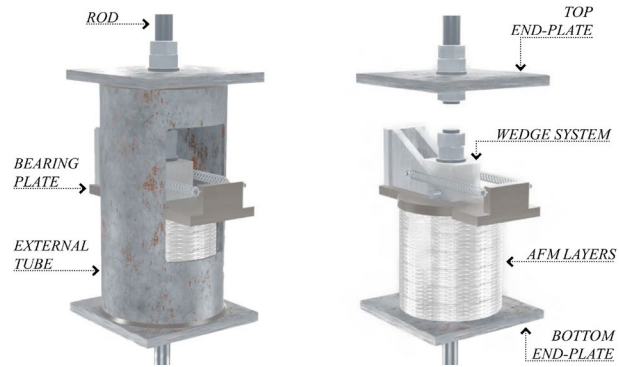


Fig. 1. Proposed metal foam damper- 3D view (a) With external tube and (b) without external tube

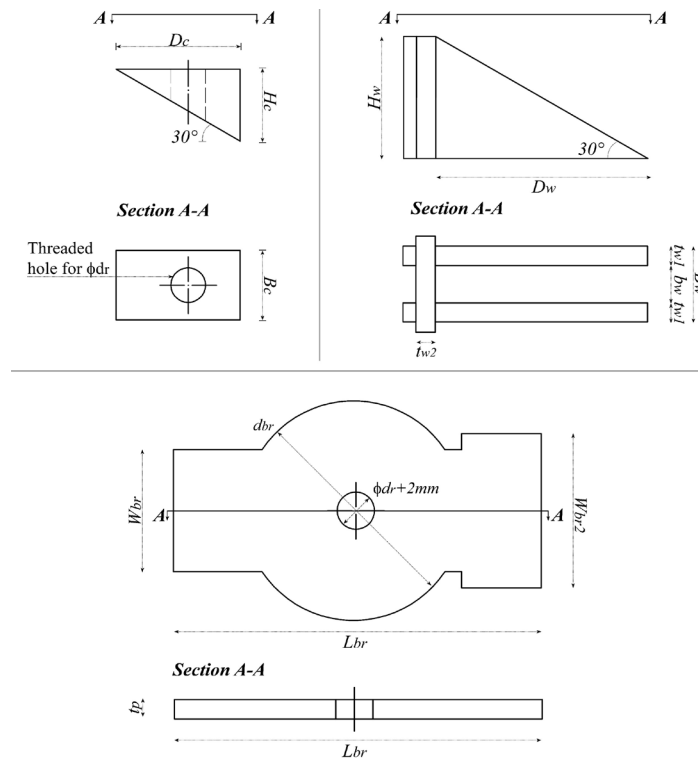


Fig. 2. Components' detail (a) Top wedge, (b) bottom wedge and (c) bearing plate

2.2 Design of the components

The design of the damper is based on the structural analysis of the equivalent conventional CBF system at the design limit state (*i.e.*, Design-Based Earthquake). Whereas the AFM will be designed

to undergo plastic deformations, the rest of the elements should remain in the elastic range during the seismic action. Thus, by following the capacity design procedure given by Eurocode 8 [10], the design axial force developed in the braces can be derived. The amplification factor considered for the design of the damper shall be determined based on the strain-hardening observed in the compression tests on the AFM (*i.e.*, 1.5).

The AFM is subjected to compressive axial forces. The required area of the AFM (A_f) is calculated based on their yield strength (f_y) and the design axial force acting in the damper (N_d), considering that the shape of each layer is cylindrical with a concentric hole to accommodate the rod. The external tube is intended to accommodate both the wedge system and the AFM layers. In order to carry out the assembly procedure of all the components, the tube has a hole on its surface. The dimensions of the opening should be large enough to allow the correct installation of the system. Therefore, the geometry of the AFM layers determines the diameter of the tube. In addition, the external tube should also be sized to remain in the elastic range under the axial forces to which it is subjected. Based on its yield strength ($f_{y,c}$) and the axial design force on the bracing amplified according to the strain-hardening of the AFM material (N_{max}), the effective area A_{ce} can be obtained. As for the wedge mechanism, the dimensions are determined depending on the rod diameter. In particular, the top wedge's dimensions (*i.e.*, B_c, D_c, H_c) are depicted in Fig. 2(a). On the other hand, the bottom wedge's dimensions (*i.e.*, $b_w, t_{w1}, t_{w2}, B_w, H_w, D_w$), shown in Fig. 2(b), should be determined to accommodate the bottom wedge horizontal displacement as a consequence of the plastic deformations of the AFM. On the other hand, the bearing plate's dimensions, depicted in Fig. 2(c), are determined to fulfil the requirements given by its dual function: to transmit the axial forces into the AFM and to accommodate the displacement of the bottom wedge. This displacement is calculated considering that when the AFM reaches the maximum stroke (δ_{max}), the corresponding horizontal displacement is equivalent to $\delta_{max}/\tan(\theta_d)$, where θ_d is the slope of the inclined surface of the wedge.

3 CASE-STUDY STRUCTURE

3.1 Design of the X-braced steel frame

Fig. 3 shows the plan and elevation views of the one-storey, three-bay by three-bay prototype steel parking building for vehicles selected for case-study purposes. The layout has a storey height of 3.50 m, while all the bays have a span length of 6 m. Seismic resistant perimeter X-type resembling CBFs are set in the -x direction, while the interior part is composed of gravity frames (with pinned beam-to-column connections and pinned column bases). Composite deck slab floors are employed, introducing a rigid horizontal diaphragm that provides stability to the overall building system. The gravity and variable loads are assumed to be uniformly distributed with values of $G_k = 4.5 \text{ kN/m}^2$ and $q_k = 2 \text{ kN/m}^2$, while the cladding load is assumed as 2.0 kN/m . The total mass of the building is equal to 92 tons and is evaluated based on the seismic combination of the Eurocode 8 [10]. The study focuses on the assessment of the bracing configuration in the -x direction. The X-brace steel structure has been designed according to Eurocode 8 recommendations, whereas the damper device has been sized by following the procedure in section 2. The seismic performance of the X-brace equipped with the damper is expected to resemble the behaviour of a buckling resistance bracing (BRB), rather than the performance presented by a conventional CBF. Therefore, the behaviour factor adopted, assuming DCH, is equal to 6.0. A Type-1 elastic response spectrum with a PGA equal to 0.35 g and soil type C has been considered to define the seismic design actions (*i.e.*, DBE) [10]. Steel S275 is employed for all structural elements. The design results are summarised in Table 1. It is important to highlight that for the considered configuration, the strength requirements at the DBE limit state govern the design while the serviceability limit state requirements are largely satisfied. Finally, the P-delta effects have not been considered since the inter-storey drift sensitivity

coefficient θ [10] resulted in being lower than 0.1 for the structure considered. By following the described procedure, the axial design force on the bracing resulted equal to 139 kN.

Table 1. Design results for the X-braced frame

One-storey structure		
Column section	Beam section	Brace circular hollow section
HE 160 B	IPE 300	114.3 x 3.2 mm

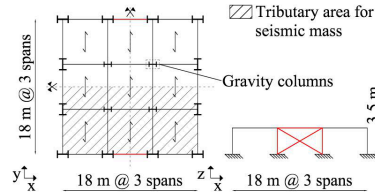


Fig. 3. Plan and elevation view of the CBF

3.2 Design of the metal foam damper

The X-brace has been upgraded with the metal foam damper considering a design action determined in section 3.1. The mechanical properties of the AFM under compression are thoroughly examined in section 4. In this regard, the yield stress of the material is assumed to be equal to 7.1 MPa, whereas the total available ductility is given by a maximum strain equal to 0.6. When introduced in the damper, the AFM is due to accommodating a maximum stroke equal to 48 mm, whereas the maximum strain expected is assumed to be 0.3. Thus, the height needed is equal to 160 mm. However, to be able to work with yield stress equal to 7.1 MPa, the height calculated (*i.e.*, 160 mm) should correspond to an already pre-squashed specimen, as indicated in section 4. Therefore, 6 AFM layers with a nominal thickness equal to 40 mm will be initially pre-compressed up to a strain of 30%. Only after that procedure, the specimen will be tested under cyclic loading.

The squared endplates, the external and inner tube, the top wedge and the bearing plate are made with S275 material, whereas the bottom wedge is made in stainless steel AISI 304. The rod is a high-strength bar M27 of 8.8 class. The external tube has a circular hollow section with diameter 195 mm and thickness 6 mm. The bearing plate and endplates have a 15 mm thickness. The elements' dimensions shown in Fig. 2 are detailed in Table 2. It is worth mentioning that the dimensions were rounded up for manufacturing purposes.

Table 2. Design results of the damper in millimeters

	Top wedge	Bottom wedge	Bearing plate		AFM	
D_c	97	29	W_{br}	95	d_c	163
B_c	54	t_{w1}, t_{w2}	$W_{br,2}$	120	d_i	34
H_c	56	B_w	d_{br}	171	l_0	40
-	-	H_w	t_p	15	-	-
-	-	D_w	L_{br}	286	-	-

4 PRELIMINARY EXPERIMENTAL TESTS AND NUMERICAL RESULTS

4.1 Sliding test on the wedge system

The wedge mechanism is aimed at accommodating the plastic deformations deriving from the squashing of the AFM in the damper after the seismic loading. If equilibrium is considered on the top and the bottom wedge under non-specific pre-load or force conditions, in order to avoid the sliding back between the members, the friction force should be bigger than the sliding component resulting from the weight of the top wedge. In this regard, Eqn 1 must be satisfied:

$$\theta_d < \tan^{-1} \mu \quad (1)$$

where θ_d is the slope of the inclined surface of the wedges and μ is the friction coefficient of the surface in-between the top and bottom wedges.

With the aim to verify that the wedge mechanism designed in section 3 fulfils Eqn. 1, a simple tilt test has been performed. The test has been simply developed by employing a small prism made in stainless steel, representing the bottom wedge, and a plate with a thermal spray coating M4, in the place of the upper wedge. The plate was kept restrained at its' right end in a way to allow the plate to rotate around that end. The prism was placed on the middle of the plate along with a digital protractor. The test consisted of manually rising the left end of the plate until the slippage of the prism occurred. As a result, the sliding of the prism arose at an angle of about 38° , whereas for a 30° angle no slippage was registered. Thus, for the geometrical and material properties given in section 3.2, no sliding should occur between the wedges under a non-specific pre-load condition.

4.2 Compression test on the aluminium foam material (AFM)

The tested samples are cut from aluminium foam panels characterised by a medium/high density, with nominal density equal to 510 kg/m^3 . The specimens have been water cut into five panels with nominal size of $90 \text{ mm} \times 90 \text{ mm} \times 40 \text{ mm}$. The panels have a closed-cell structure characterised with a variable dimension of the cells and a rather inhomogeneous distribution of the cell size.

The tests have been carried out at the STRENGTH laboratory at the University of Salerno. The aim was to determine the main mechanical properties of the AFM in the relevant direction of resistance, arranged in two configurations, a single-layer and a four-layer one (Fig. 4). Metal foams are usually orthotropic materials due to the production process, which includes a lamination of the material with a rolling machine after foaming. The tests herein presented have been executed in transverse compression. The specimens have a cross-section of about $90 \times 90 \text{ mm}$. Both tests have been executed under displacement control in quasi-static conditions, imposing a velocity equal to 2 mm/min . The machine used is a universal testing machine Schenck Hydropuls S56. The testing equipment is constituted of a hydraulic piston with a loading capacity equal to $\pm 630 \text{ kN}$, maximum stroke equal to $\pm 125 \text{ mm}$ and a self-balanced steel frame used to counteract the axial loadings. To measure the axial displacements, the testing device is equipped with 4 LVDTs. The average displacement among the data given by LVDTs shall be used in further calculations. Moreover, the tension/compression loads are measured through a load cell.

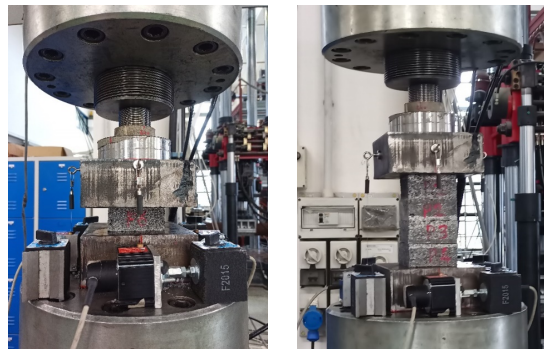


Fig. 4. AFM compression test configurations (a) Single-layer and (b) four-layer

The data obtained have been processed with the aim of representing the stress-strain curves for both the arrangements. The results, depicted in Fig. 5, show that in both configurations, the material is characterised by an initial elastic response until the yield of the material is reached. Subsequently, a strain-hardening phase is observed, which is attributed to the densification of the material during

the squashing. However, whereas the single-layer arrangement (Fig. 5 (a)) presents a significant increase in strength after a 40% strain level, the four-layer one does not (Fig. 5 (b)). The steep rise of the strength in the single-layer configuration is attributed to the restraint condition of the specimen. On the other hand, the stiffness during the strain-hardening phase in the four-layer arrangement test is stable enough to represent the specimens' behaviour through a by-linear model. It was also observed that the coupons that constitute such configuration did not deform equally during the test, which could be related to the randomness of the metal foams' properties.

Both tests were carried out by introducing an unloading and subsequent reloading sequence at a certain point to enable the evaluation of the stiffness of the metal foam specimens. The initial stiffness, derived from the first loading phase, resulted in being much lower than the one obtained during the reloading phase (Fig. 5). This variation can also be explained by the increase of density during the progressive squashing phenomena.

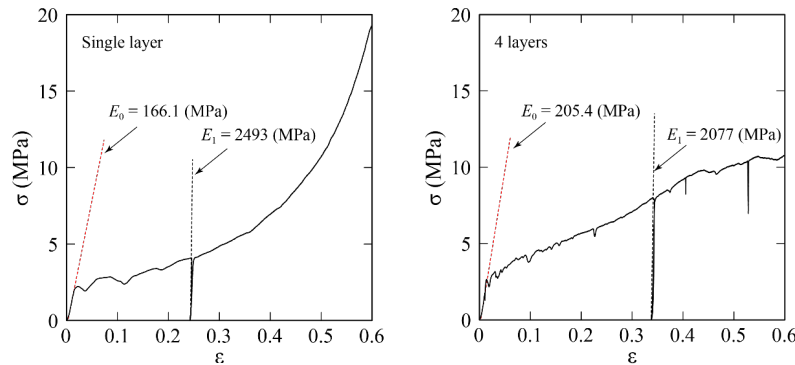


Fig. 5. AFM compression test (a) Single-layer and (b) four-layer configurations

The design of the damper presented in section 3 has been carried out by considering the properties determined in the four-layer test. In particular, the values considered are derived from a pre-squash procedure aimed at increasing both the yield stress of the material and the elastic modulus. The pre-hardening procedure consists of (1) pre-loading of the AFM up to a strain level of about 30%. The stress corresponding to that strain level (*i.e.*, 7.1 MPa) is the yield stress of the foam. Subsequently, (2) unloading up to a strength value equal to zero. This point will be subsequently considered the new origin of the stress-strain diagram. Finally, (3) reloading of the specimen up to a total strain equal to 60%. The stress corresponding to that strain level (*i.e.*, 10.8 MPa), is the maximum stress the AFM can be subjected to. Through this procedure, the rise of the elastic modulus of the AFM reaches a value about ten times higher than the initial one, providing the device with sufficient stiffness.

4.3 ABAQUS simulation

To evaluate the behaviour of the device, a Finite Element Model has been developed in Abaqus. The set-up of the FE model consists of a series of steps: defining the geometry of the elements, modelling the material properties, defining the boundary conditions and choosing the element type and mesh size. The objective is to define a solid three-dimensional model constituted by the external tube, the endplates, the bearing plate, the AFM layers, the top and bottom wedges and the springs (Fig. 6). Regarding the geometry, the plates have been defined through extrusion of their cross-section, while the external tube and the AFM layers have been defined by revolving half their vertical section around their axis. The material properties were subsequently introduced. The AFM

layers have been defined through inelastic properties considering the results of the experimental test given in section 4.2, whereas the external tube, the wedges and the plates have been defined as elastic ones. The springs are characterized by a stiffness of 2 N/mm and are pre-elongated 70 mm before the analysis. The interaction between the elements has been defined according to a surface-to-surface formulation with finite sliding. In the normal direction a “hard contact” has been used, while in the tangential direction a friction coefficient equal to 0.6 has been adopted for the contact between the top and bottom wedges and 0.2 has been assumed for the rest of the surfaces in contact.

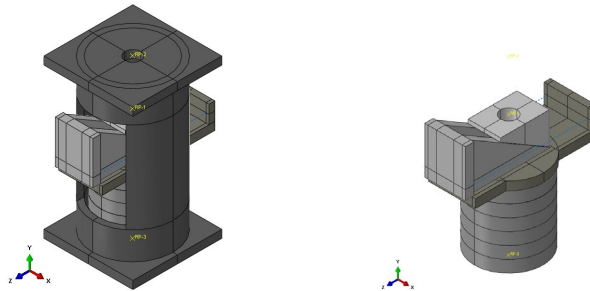


Fig. 6. Finite element model (a) whole model (b) Foam and wedge device only

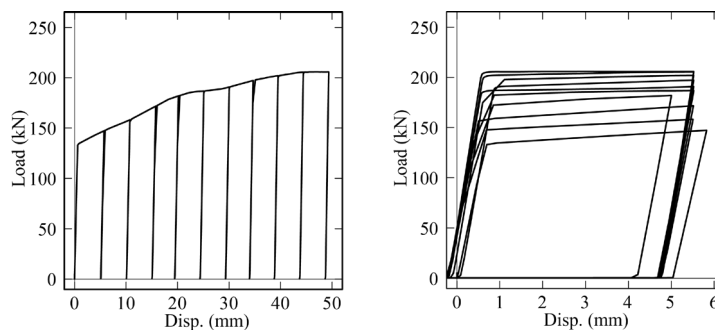


Fig. 7. Analysis results- Force-displacement curve (a) Bearing plate (b) Top wedge

The FE model has been analyzed by applying a boundary condition to the top wedge with a cyclical history characterized by a constant amplitude of 5 mm, leading to a total stroke of 50 mm in the AFM layers. The movement of the bottom wedge increases progressively until the last cycle, in which the movement is evident. Fig. 7(a) shows the analysis results in terms of force-displacement curves regarding the bearing plate, whereas Fig. 7(b) represents the curve corresponding to the top wedge. The results shown in (a) illustrate the displacement accumulation during the cycles up to 50 mm. The progressive displacement of the bearing plate is the one expected, as the plastic deformations are absorbed by the wedge system in each cycle. In fact, the curve in (b) demonstrates the correct activation of the wedge system. Once the gap between the top and bottom wedge is generated, the pre-elongated springs pull the bottom wedge to accommodate the vertical displacements. No pinching behaviour is registered. The curve presents a flag-shape behaviour.

5 CONCLUSIONS

The present work presents a metal foam damper intended to be introduced in the bracing component of an X-braced steel structure. The device consists of aluminium foam layers, able to dissipate the

incoming seismic energy, and a wedge system equipped with a spring mechanism, with the aim to absorb the permanent deformations following the seismic actions. With the objective of studying the behaviour of the device under seismic loading, preliminary experimental and numerical tests have been performed on the single components. The results obtained enable to settle the mechanical properties that characterise the aluminium foam material in compression. In addition to confirming its high ductility capacity under compression, it was determined that a pre-hardening procedure shall be needed to provide the AFM with a high enough strength and elastic modulus to provide the damper with enough stiffness. On the other hand, the geometry and thermal treatment adopted in the design of the wedge mechanism assure the proper functioning of the system. Given these results, along with the numerical simulations, the device is expected to present stable hysteretic loops under cyclic loading conditions. Pinching behaviour under cyclic loading conditions shall be avoided by introducing the device in the brace of an X-braced frame.

ACKNOWLEDGMENT

The authors thank the Ministry of Foreign Affairs and International Cooperation for funding the project PGR07413- "Advanced Materials for Light and Sustainable Constructions in Seismic Zones". The project is being developed within the framework of the "Executive Programme of Cooperation in the Field of Science and Technology between the government of Italy and Japan for the period 2020-2022".

REFERENCES

- [1] Latour M., Rizzano G., D'Aniello M., Landolfo R., Babesan N., Flexural behaviour of double-skin composite steel-aluminium foam sandwich panels. XXVII Congresso C.T.A., 2019.
- [2] Boomsma K., Poulidakos D., Zwick F., Metal foams as compact high-performance heat exchangers, *Mechanics of Materials*, Volume 35, Issue 12, 1161-1176, 2003.
- [3] Banhart J., *Manufacture, characterization and application of cellular metals and metal foams*, *Progress in Materials Science*, Volume 46, Issue 6, 559-632, 2001.
- [4] Ashby M.F., Evans A.G., Fleck N.A., Gibson L.J., Hutchinson J.W., Wadley H.N.G., *Metal Foams: A design Guide*. Editor: Butterworth and Heinemann, 2000.
- [5] Lefebvre LP., Banhart J., Dunand C., *Porous Metals and Metallic Foams: Current Status and Recent Developments*, *Advanced Engineering Materials*, Volume 10, Issue 9, 2008
- [6] Smith B.H., Szyniszewski S., Hajjar J.F., Schafer B.W., Arwade S.R., *Steel foam for structures: A review of applications, manufacturing and material properties*, *Journal of Constructional Steel Research*, Volume 71, 1-10, 2012.
- [7] Moradi M., *Structural applications of metal foams considering material and geometrical uncertainty*, PhD Thesis, University of Massachusetts Amherst, 2011.
- [8] Moradi M., Arwade S.R., *Structural Engineering Mechanics*, 51(6): 1017-1036, 2014.
- [9] Tamai H., Takamatsu T., *Cyclic loading test on a non-compression brace considering performance based-seismic design*, *JCSR*, 61: 1301-1317, 2005.
- [10] EN 1998-1: *Design of structures for earthquake resistance- Part 1: General rules, seismic actions and rules for buildings*, European Committee for Standardization, Brussels.
- [11] Ferrante Cavallaro G., Francavilla A., Latour M., Piluso V., Rizzano G., *Experimental behaviour of innovative thermal spray coating materials for FREEDAM joints*.

KEYWORDS

Metal-foam, Damper, Steel structures, Concentrically braced frames